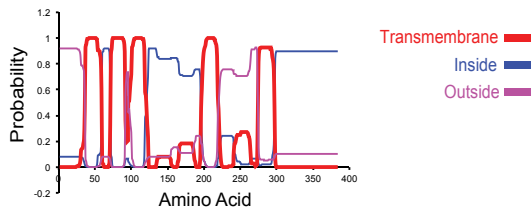


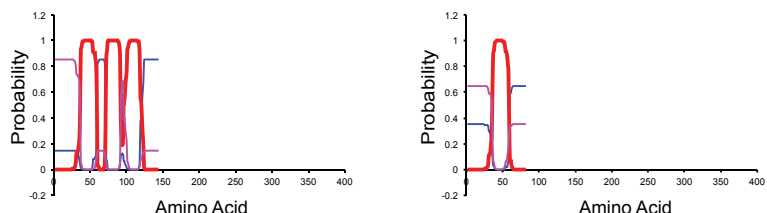
**Fig. S1. osta-1 encodes a neuronally expressed member of a conserved transmembrane protein family.** (A) Phylogenetic analyses of OSTA-1 and related protein sequences. Analyses were performed by MUSCLE alignment followed by PHYML analysis for estimating maximum likelihood phylogenies. Scale bar indicates the number of amino acid changes per site. Sequences were obtained from the NCBI protein database. *Hs*, *Homo sapiens*; *Dm*, *Drosophila melanogaster*; *Ce*, *C. elegans*; *Cr*, *Chlamydomonas reinhardtii*; *Mm*, *Mus musculus*. For a detailed phylogenetic analysis, see [http://uswest.ensembl.org/Homo\\_sapiens/Gene/Compara\\_Tree?g=ENSG00000163959](http://uswest.ensembl.org/Homo_sapiens/Gene/Compara_Tree?g=ENSG00000163959). (B) Predicted transmembrane helix sequences and di-leucine targeting motifs in OSTA-1 and related proteins. Residues of transmembrane domains are underlined. Possible di-leucine targeting motifs are indicated in red. (C) Expression of *gfp* under 2.1 kb of *osta-1* upstream regulatory sequences in a transgenic adult hermaphrodite. Expression in head and tail sensory neurons is indicated by white and yellow arrows, respectively. Anterior is at left. (D) Expression of *osta-1*-related *C. elegans* genes. Only expression in the head is shown. The image of F40E10.6 expression is a composite of three images acquired from the same animal. The strain expressing a F40E10.6::gfp fusion gene was a kind gift from I. Hope (University of Leeds) (Dolphin and Hope, 2006). *osta-2* and *osta-3* transcriptional expression constructs were generated by PCR fusion of *gfp* sequences to 3.2 kb and 3.1 kb upstream regulatory sequences, respectively. (E) Expression of OSTA-1::mCherry driven under cell-specific promoters. Scale bars: 0.2 μm in C; 10 μm in D,E.

*osta-1* wild type



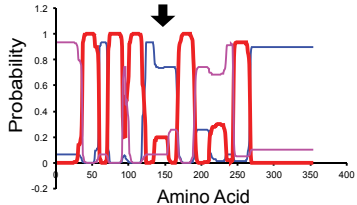
*osta-1(tm5255)*

5/6 1/6

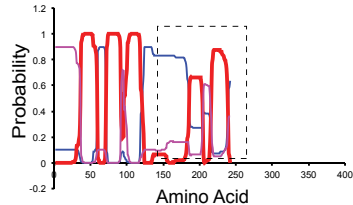


*osta-1(ttTi4182)*

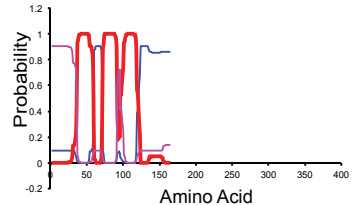
3/7



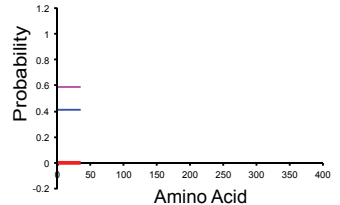
2/7



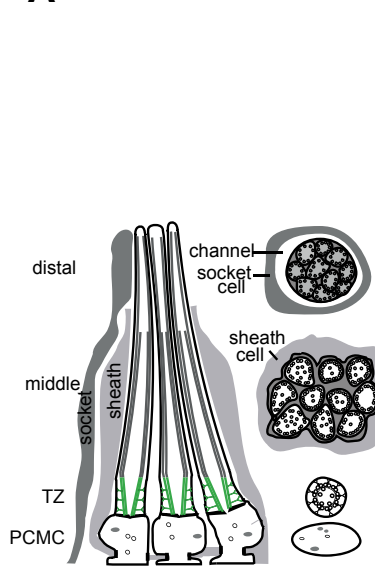
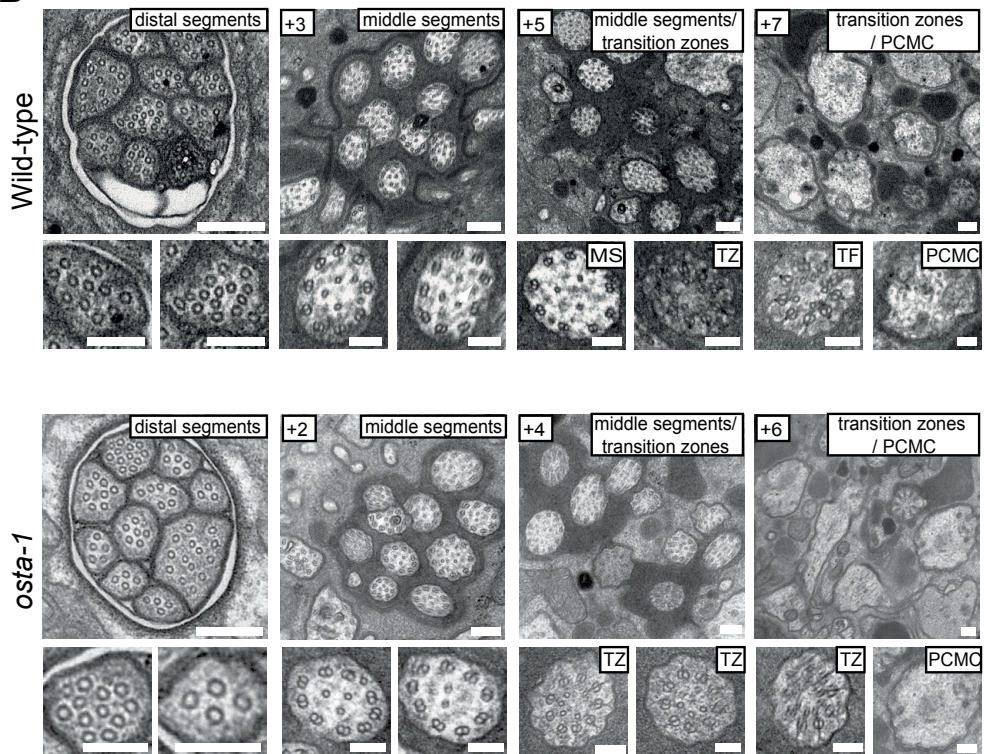
1/7



1/7



**Fig. S2. Transmembrane topologies of OSTA-1 proteins predicted to be encoded by cDNAs isolated from the indicated *osta-1* mutant strains.** Five out of six and one out of six cDNAs isolated from *tm5255* mutants are predicted to encode proteins truncated after the third or first transmembrane domains, respectively. Four different *osta-1* cDNA isoforms were isolated from *ttTi4182* mutants. In 3/7 isolates, the first 24 bp of exon 5 were spliced to exon 6 resulting in a protein remaining in frame but lacking residues between the third and fourth transmembrane helices (arrow). In 2/7 isolates, the first 11 bp of the *Mos1* transposon were spliced to exon 6; these isoforms are predicted to encode a protein that is out of frame after the third transmembrane domain (boxed residues). In 1/7 isolates, a 38 bp deletion in exon 5 is predicted to result in a premature stop codon in the fifth exon and protein truncation after the third transmembrane domain. Finally, 1/7 isoforms retained the first intron, the first 48 bp of exon 5, and the first 11 bp of the *Mos1* transposon spliced to exon 6; this isoform is predicted to encode a protein truncated before the first transmembrane helix. Topologies were computed via TMHMM analysis (Krogh et al., 2001) (<http://www.cbs.dtu.dk/services/TMHMM/>). Plots show posterior probabilities for the inside/outside/transmembrane domains.

**A****B****C**

	Wild-type	osta-1
Distal segments (DS) <sup>1</sup>	average axoneme number in distal pore	10 (n=4)
	average MT singlet number / DS <sup>5</sup>	8 (n=44)
	axonemes with no microtubules	0
Middle segments (MS) <sup>2</sup>	average axoneme number in mid pore region	12 (n=4)
	average MT doublet number / MS <sup>5</sup>	9 (n>100)
	axonemes with abnormal accumulations	0
Transition zones (TZ) <sup>3</sup>	average diameter of surrounding membrane (nm) / TZ	260 ± 40 (n=34)
	% TZs with enlarged membrane diameters	0 (n=34)
	% TZs with Y-links	100 (n>12)
Periciliary membrane compartments (PCMC) <sup>4</sup>	% PCMCs with abnormal accumulations	0
	PCMC transverse area / μm <sup>2</sup>	0.44 ± 0.24 (n=73)
		0.50 ± 0.14 (n=12)

<sup>1</sup> distal region of axonemes (~ 3 μm) containing only singlet microtubules

<sup>2</sup> proximal region of axonemes (~3 μm) containing doublet microtubules

<sup>3</sup> Most proximal region of axonemes (~ 1 μm), where doublet & singlet microtubules are drawn together by an internal apical membrane and where MT doublets are linked to ciliary membrane via Y-links.

<sup>4</sup> PCMC; periciliary membrane compartment (~0.5 μm<sup>2</sup>) that exists immediately below the ciliary axonemes

<sup>5</sup> as analyses were performed on serial sections, the same axoneme may have been counted more than once

**Fig. S3. Ultrastructure of amphid channel cilia in *osta-1* mutants. (A)** The ultrastructural organization of amphid channel cilia. **(B)** Low (above) and high (below) magnification images of amphid channel sensory cilia from TEM serial cross-sections of the amphid pore in wild-type and *osta-1* (*ttTi4182*) animals. Boxed numbers at upper left denote proximal positioning of sections relative to the most distal section (leftmost panels). Similar to wild-type worms, the amphid pore of *osta-1* mutants contains ten ciliary axonemes, each consisting of a distal segment (singlet microtubules), a middle segment (doublet microtubules), and a transition zone (ring of doublet microtubules drawn together by the apical ring and connected to the ciliary membrane via Y-links). The ciliary base of *osta-1* worms also appears normal, containing transitional fibers and a grossly normal periciliary membrane compartment. MS, middle segment; TZ, transition zone; TF, transition fibers; PCMC, periciliary membrane compartment. Nematode fixation, embedding and transmission electron microscopy of amphid channel cilia were performed as previously described (Williams et al., 2011). Scale bars: 200 nm in low magnification images; 100 nm in high magnification images. **(C)** Quantification of amphid channel cilium ultrastructural features in wild-type and *osta-1* mutants.

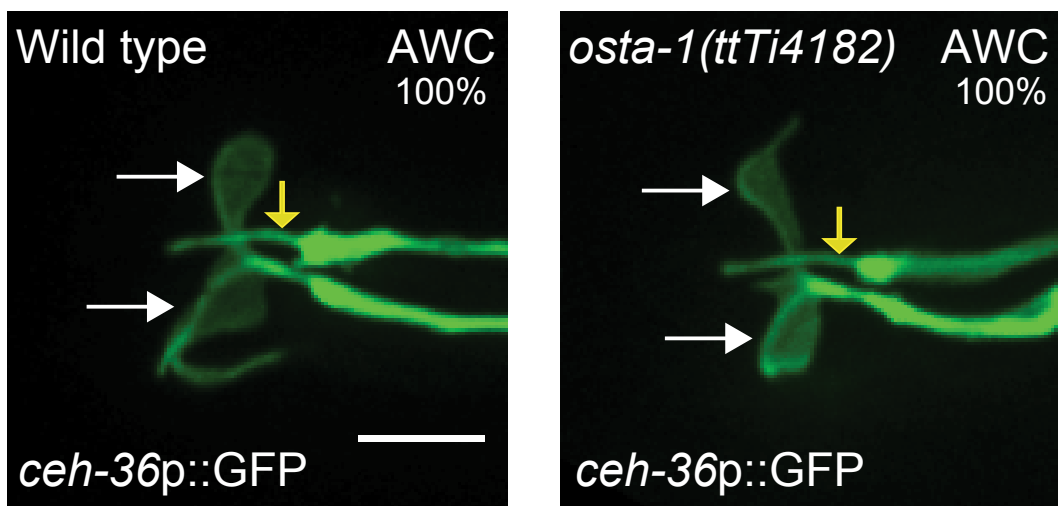
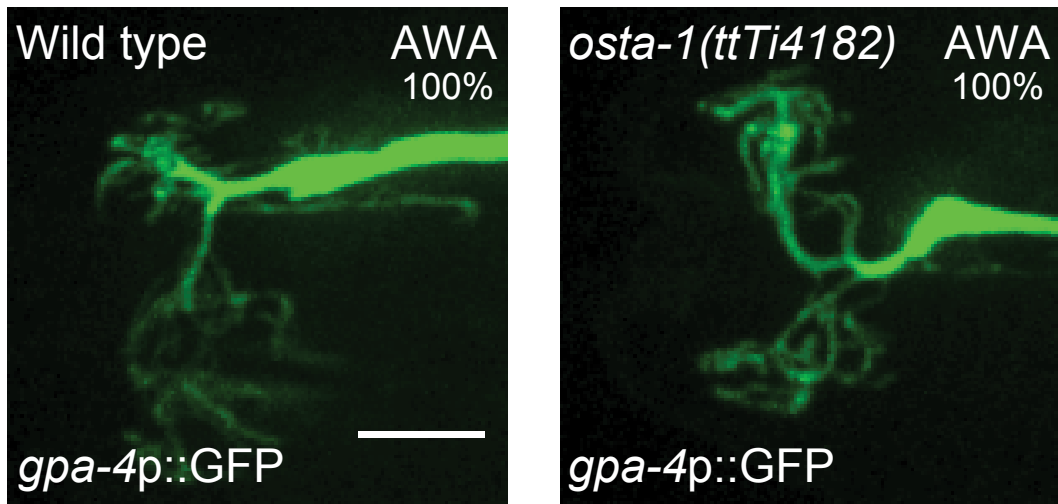
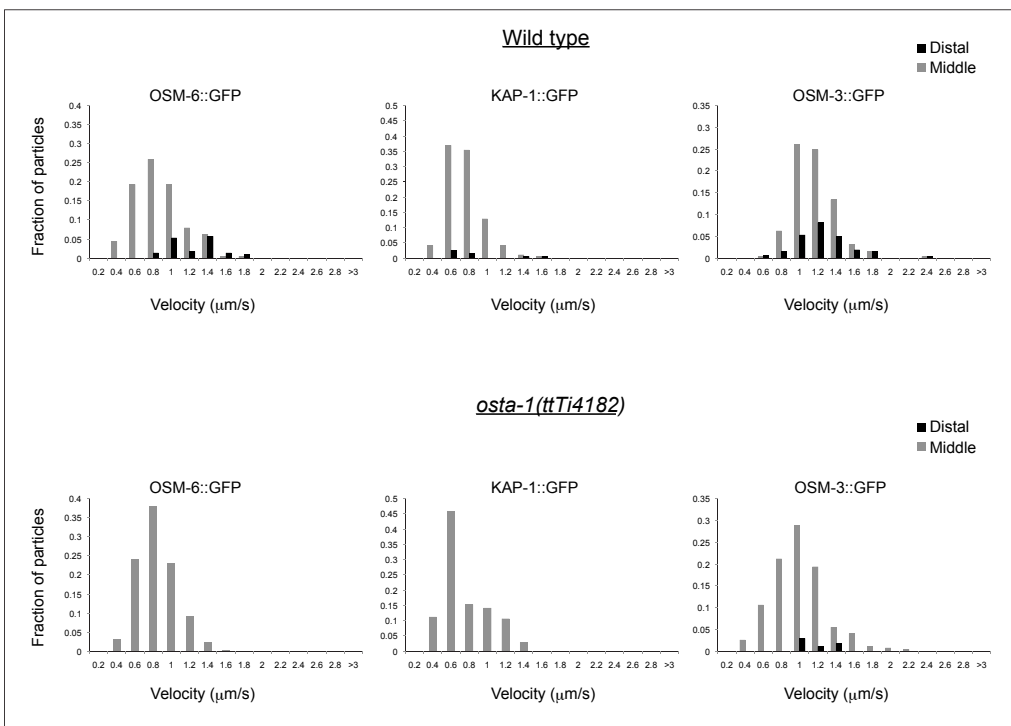


**Fig. S4. Overall morphology of the AWA and AWC cilia is unaffected in *osta-1(ttTi4182)* mutants.** White and yellow arrows indicate AWC and ASE cilia, respectively. Numbers at top right indicate percentage of cilia exhibiting the phenotype;  $n \geq 25$  each. Scale bar: 5  $\mu$ m.

### AWB



### ASH

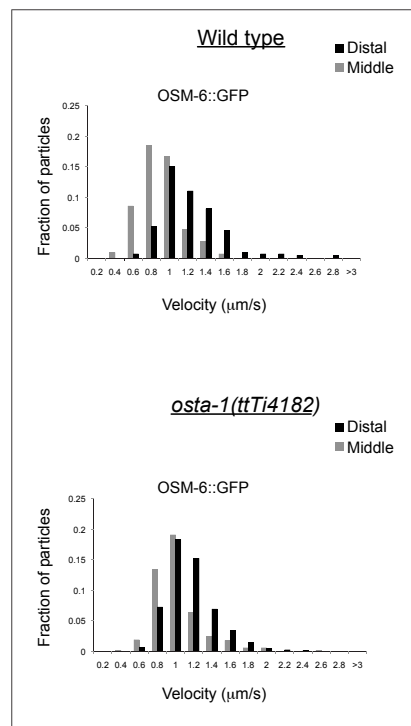


**Fig. S5. Anterograde IFT velocities in AWB and ASH cilia in wild type and *osta-1* mutants.** Fusion proteins were expressed under the *str-1* (AWB) or *sra-6* (ASH/ASI) promoters. Velocities of indicated fusion proteins in the middle and distal segments are indicated by gray and black bars, respectively. Numbers of particles and kymographs analyzed and statistical analyses are shown in Table 2.

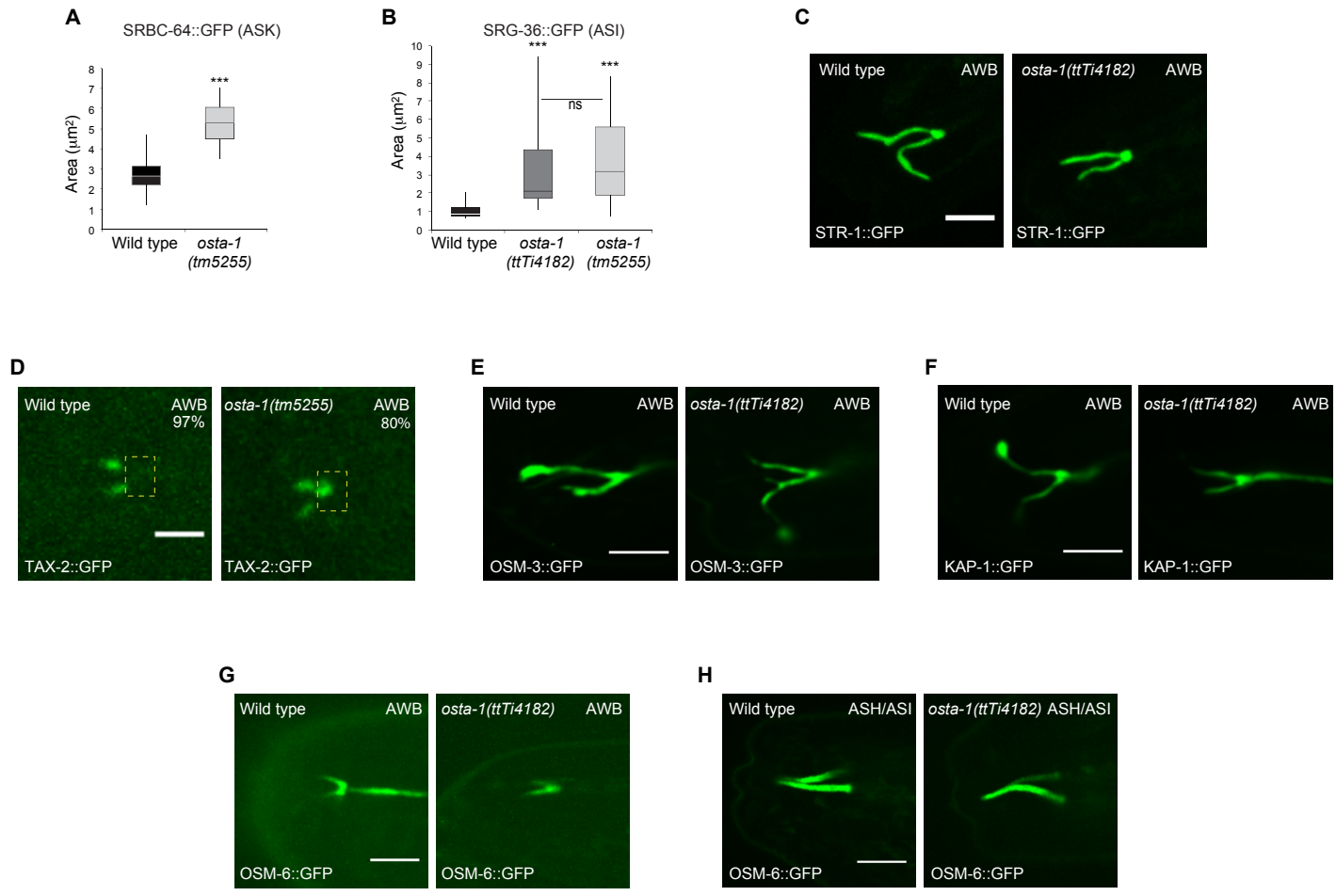


**Fig. S6. Localization of subsets of ciliary transmembrane and IFT proteins in *osta-1* mutants.** (A,B) Localization of SRBC-64::GFP in ASK (A) and of SRG-36::GFP in ASI (B) in the indicated genetic backgrounds. Measurements were performed as described in the legend to Fig. 4A,B.  $n=40$  each; outliers (values greater or less than three standard deviations from the mean) are not shown. Adult animals were grown at 20°C. \*\*\* $P<0.001$ , versus wild type. ns, not significant. (C-H) Localization of the indicated fusion proteins in AWB (C-G) and ASH/ASI (H) in the indicated genetic backgrounds. Expression was driven in AWB and ASH/ASI under the *str-1* and *sra-6* promoters, respectively. Numbers at top right (D) indicate percentage of cilia exhibiting the phenotype;  $n\geq 20$  each. Images in C and D were created by maximum  $z$ -projections, whereas images in E-H were created by projecting individual 1-minute time-lapse movies taken in a single focal plane. Adult animals were grown at 20°C. Scale bars: 2.5  $\mu\text{m}$  in D; 5  $\mu\text{m}$  in C,E-H.

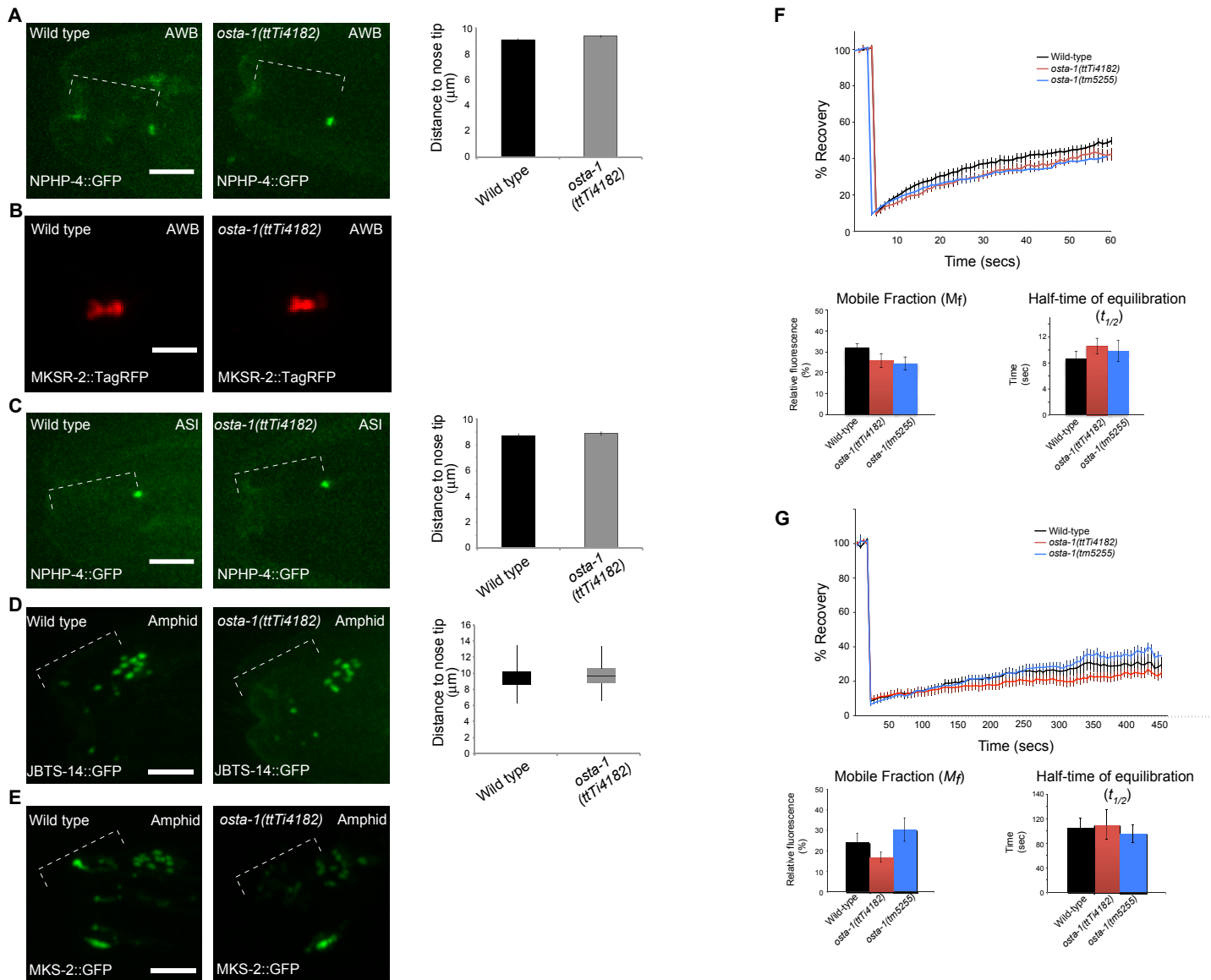


**Fig. S7. Mutations in *osta-1* do not compromise the periciliary diffusion barrier.** (A-E) Localization of transition zone fusion proteins in AWB (A,B), ASI (C), or in multiple ciliated head sensory neurons (D,E) in the indicated genetic backgrounds. Scale bars: 5  $\mu\text{m}$ . Shown to the right is the quantification of fusion protein localization or distribution relative to the tip of the animal's nose. Expression in AWB and ASI was driven under the *str-1* and *srg-47* promoters, respectively; expression in multiple sensory neurons was driven under endogenous or ciliated neuron-specific promoters (Huang et al., 2011).  $n=15-20$  animals each. Animals were grown at 20°C. (F,G) Kinetics of fluorescence recovery following photobleaching of SRG-36::GFP signals in ASI cilia in the indicated strains expressing the *srg-36::gfp* transgene driven under the *str-3* promoter. SRG-36::GFP photobleaching was performed within an intraciliary region (F) or along the entire ASI cilium (G). A single cilium per animal was analyzed.  $n=10-12$  cilia analyzed per genotype and condition. Error bars indicate s.e.m. Wild-type and mutant  $M_f$  and  $t_{1/2}$  values are not significantly different in F or G (ANOVA and post-hoc corrections for multiple comparisons). Intracilia bleach:  $M_f$  both *osta-1* alleles different from wild-type at  $P>0.1$ ;  $t_{1/2}$ , both *osta-1* alleles different from wild-type at  $P>0.8$ . Entire cilium bleach:  $M_f$  both *osta-1* alleles different from wild-type at  $P>0.9$ ;  $t_{1/2}$ , both *osta-1* alleles different from wild-type at  $P>0.7$ .

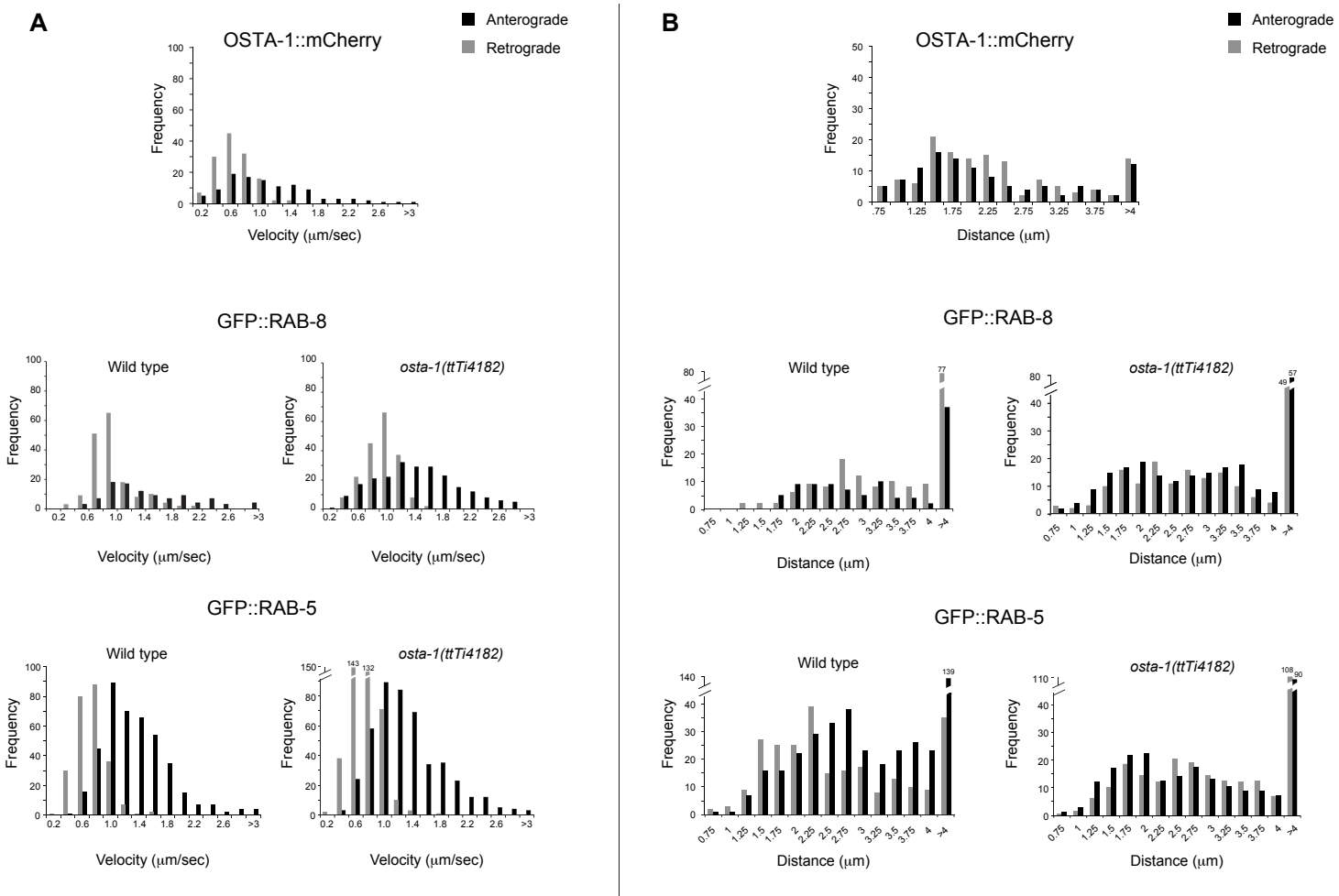
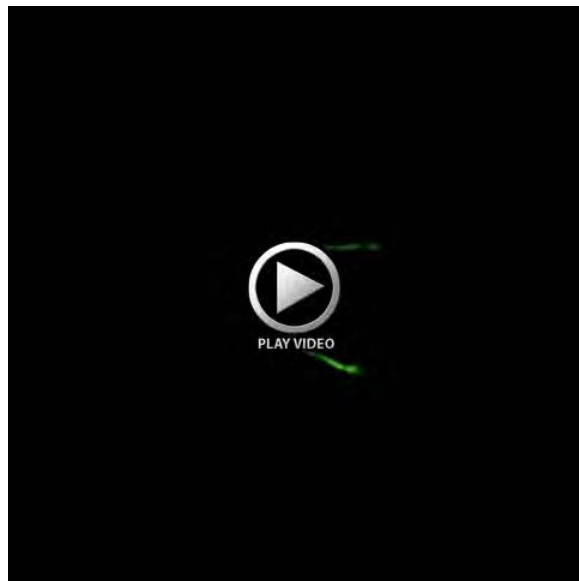
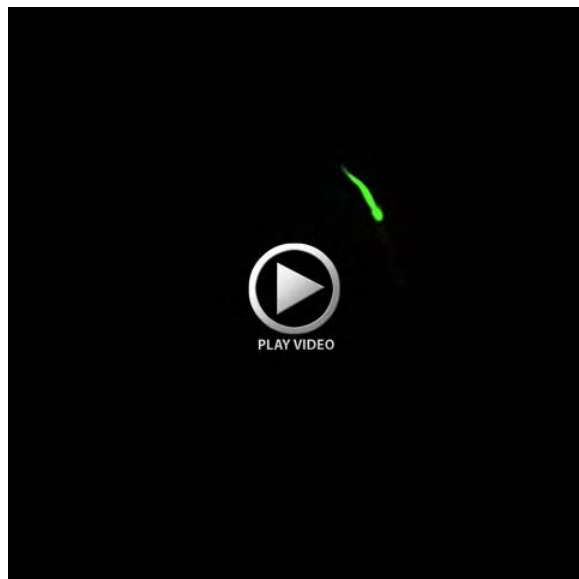


**Fig. S8. Fusion protein velocities and track lengths in AWB dendrites.** (A) Fusion protein velocities. (B) Track lengths.  $n=81-468$  particles; 7-15 animals per strain.



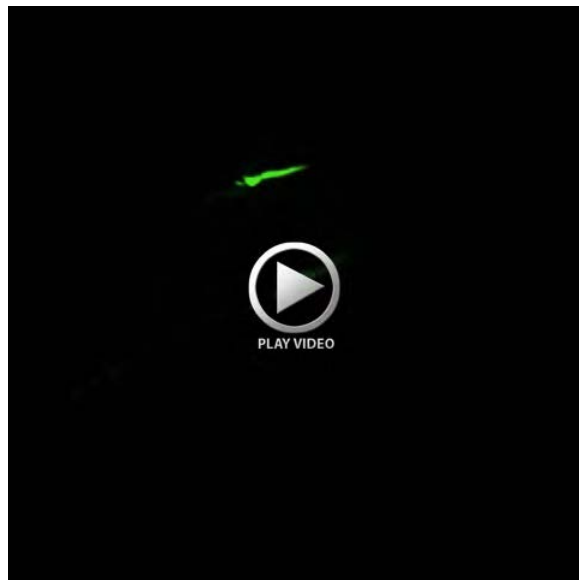
**Movies 1, 2. FRAP of an intraciliary region of the ASI cilium expressing SRG-36::GFP under the *str-3* promoter in wild-type or *osta-1(ttTi4182)* animals.** Images of wild-type (Movie 1; cilium at bottom) or *osta-1(ttTi4182)* (Movie 2) animals were acquired every second for 60 seconds with an exposure of 100 msec. Animals were grown at 20°C.



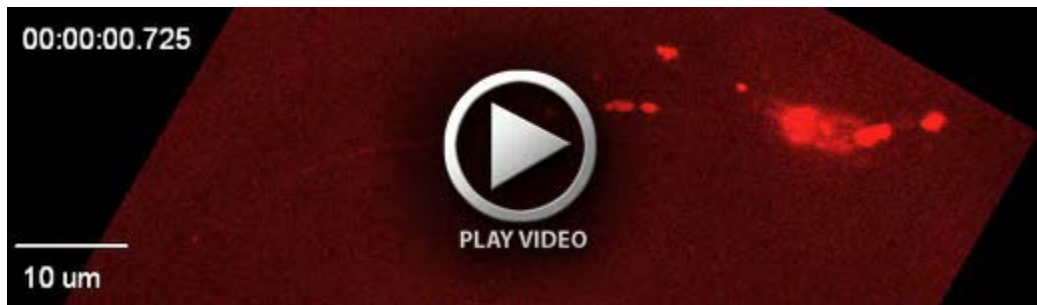
**Movies 1, 2. FRAP of an intraciliary region of the ASI cilium expressing SRG-36::GFP under the *str-3* promoter in wild-type or *osta-1(ttTi4182)* animals.** Images of wild-type (Movie 1; cilium at bottom) or *osta-1(ttTi4182)* (Movie 2) animals were acquired every second for 60 seconds with an exposure of 100 msec. Animals were grown at 20°C.



**Movies 3, 4. FRAP of the whole ASI cilium expressing SRG-36::GFP under the *str-3* promoter in wild-type or *osta-1(tm5255)* animals.** Images of wild-type (Movie 3) or *osta-1(tm5255)* (Movie 4; cilium at left) animals were acquired every 5 seconds for 600 seconds with an exposure of 100 msec. Animals were grown at 20°C.



**Movies 3, 4. FRAP of the whole ASI cilium expressing SRG-36::GFP under the *str-3* promoter in wild-type or *osta-1(tm5255)* animals.** Images of wild-type (Movie 3) or *osta-1(tm5255)* (Movie 4; cilium at left) animals were acquired every 5 seconds for 600 seconds with an exposure of 100 msec. Animals were grown at 20°C.



**Movie 5. A subset of OSTA-1::mCherry proteins is mobile in the AWB dendrite.** Movie is shown at 4.5× real time. Animals were grown at 25°C.

**Table S1. Strains used in this work**

Strain	Genotype	Source
PY1058	<i>oyIs14[sra-6p::gfp]</i> V	(Sarafi-Reinach et al., 2001)
PY1089	<i>kyIs104[str-1p::gfp]</i> X	(Troemel et al., 1997)
PY3453	<i>oyIs50[ceh-36p::gfp]</i>	(Kim et al., 2010)
PY4527	<i>kyIs156[str-1p::odr-10 cDNA::gfp]</i> X	(Dwyer et al., 2001)
PY4575	<i>kyIs104[str-1p::gfp] odr-1(n1936)</i> X	(Mukhopadhyay et al., 2008)
PY4640	Ex[srbc-64p::srbc-64::gfp; unc-122p::dsRed]	(Kim et al., 2009)
PY5495	Ex[srbc-66p::gfp, unc-122p::dsRed]	(Kim et al., 2009)
PY5587	Ex[str-1p::kap-1::gfp; unc-122p::dsRed]	(Mukhopadhyay et al., 2007)
PY5593	<i>bbs-8(nx77)</i> V; <i>kyIs104[str-1p::gfp]</i> X	(Mukhopadhyay et al., 2008)
PY6101	<i>oyIs61[gpa-4pdel::gfp]</i>	Woong Kim and P.S. (unpublished)
PY6735	Ex[sra-6p::osm-6::gfp; unc-122p::dsRed]	(Mukhopadhyay et al., 2007)
PY6959	Ex[str-1p::str-1 cDNA::gfp; unc-122p::dsRed]	(Mukhopadhyay et al., 2008)
PY6967	<i>rab-8(tm2526)</i> I; <i>kyIs104[str-1p::gfp]</i> X	(Mukhopadhyay et al., 2008)
PY7141	Ex[str-1p::osm-6::gfp; unc-122p::dsRed]	(Mukhopadhyay et al., 2007)
PY7173	<i>osta-1(oy98)</i> II	This work
PY7175	Ex [C01B12.4 translational fusion::gfp; unc-122p::dsRed]	This work
PY7177	Ex[C01B12.4p::gfp; unc-122p::dsRed]	This work
PY7346	Ex[srd-23p::gfp::rab-8 cDNA; unc-122p::dsRed]	(Kaplan et al., 2012)
PY7350	Ex[srd-23p::gfp::rab-5 cDNA; unc-122p::dsRed]	David Doroquez and P.S. (unpublished)
PY8178	Ex[str-1p::tax-2::gfp; unc-122p::dsRed]	(Mukhopadhyay et al., 2008)
PY8182	Ex[srbc-66p::tax-2::gfp; srbc-66p::che-13::TagRFP; unc-122p::gfp]	This work
PY8621	Ex[srbc-66p::C01B12.4 cDNA::mCherry; nphp-4::npbp-4::gfp; unc-122p::gfp]	This work
PY8624	<i>osta-1(ttTi4182)</i> II; Ex[srbc-66p::gfp, unc-122p::dsRed]	This work
PY8625	<i>osta-1(ttTi4182)</i> II; <i>oyIs14[sra-6p::gfp]</i> V	This work
PY8628	<i>osta-1(ttTi4182)</i> II; <i>kyIs104[str-1p::gfp]</i> X	This work; <i>ttTi4182</i> allele from NemaGENETAG Consortium
PY8629	<i>osta-1(ttTi4182)</i> II; Ex[srbc-66p::C01B12.4 cDNA::mcherry; unc-122p::gfp]	This work
PY8630	<i>osta-1(ttTi4182)</i> II; <i>oyIs61[gpa-4pdel::gfp]</i>	This work
PY8631	<i>osta-1(ttTi4182)</i> ; Ex[C01B12.4p::C01B12.4::gfp; unc-122p::dsRed]	This work
PY8637	<i>osta-1(ttTi4182)</i> II; Ex[srbc-64p::srbc-64::gfp; unc-122p::dsRed]	This work
PY8638	<i>osta-1(ttTi4182)</i> II; Ex[str-1p::str-1 cDNA::gfp; unc-122p::dsRed]	This work
PY8639	<i>osta-1(ttTi4182)</i> II; Ex[str-1p::osm-6::gfp; unc-122p::dsRed]	This work
PY8640	<i>osta-1(ttTi4182)</i> II; <i>oyIs50[ceh-36p::gfp]</i>	This work
PY8643	<i>osta-1(ttTi4182)</i> II; Ex[str-1p::kap-1::gfp; unc-122p::dsRed]	This work
PY8644	<i>osta-1(ttTi4182)</i> II; <i>kyIs156[str-1p::odr-10 cDNA::gfp]</i> X	This work
PY8646	<i>osta-1(ttTi4182)</i> II; Ex[sra-6p::osm-6::gfp; unc-122p::dsRed]	This work
PY8647	<i>osta-1(ttTi4182)</i> II; <i>dpy-23(e840)</i> <i>kyIs104[str-1p::gfp]</i> X	This work

PY8649	Ex [ <i>str-1p::osm-3b::gfp; unc-122p::dsRed</i> ]	(Mukhopadhyay et al., 2007)
PY8651	<i>osta-1(ttTi4182) II; kyIs104[str-1p::gfp] odr-1(n1936) X</i>	This work
PY8652	<i>osta-1(ttTi4182) II; Ex[C01B12.4 PCR fragment; unc-122p::dsRed]</i>	This work
PY8653	<i>rab-8(tm2526) I; osta-1(ttTi4182) II; kyIs104[str-1p::gfp] X</i>	This work
PY8655	<i>osta-1(ttTi4182) II; Ex[str-1p::osm-3b::gfp; unc-122p::dsRed]</i>	This work
PY8656	<i>osta-1(ttTi4182) II; Ex[srd-23p::gfp::rab-8 cDNA; unc-122p::dsRed]</i>	This work
PY8657	<i>osta-1(ttTi4182) II; bbs-8(nx77) V; kyIs104[str-1p::gfp] X</i>	This work
PY8663	<i>osta-1(ttTi4182) II; Ex[str-3p::srg-36 cDNA::gfp; elt-2p::gfp]</i>	This work
PY8665	<i>osta-1(ttTi4182) II; Ex[srd-23p::gfp::rab-5 cDNA; unc-122p::dsRed]</i>	This work
PY8666	<i>Ex[str-3p::srg-36 cDNA::gfp; elt-2p::gfp]</i>	(McGrath et al., 2011)
PY8673	<i>Ex[str-1p::C01B12.4 cDNA::mCherry; unc-122p::gfp]</i>	This work
PY8674	<i>osta-1(ttTi4182) II; Ex[str-1p::tax-2::gfp; unc-122p::dsRed]</i>	This work
PY8677	<i>osta-1(tm5255) II; kyIs104[str-1p::gfp] X</i>	This work; <i>tm5255</i> allele from S. Mitani
PY8679	<i>osta-1(ttTi4182) II; Ex[srbc-66p::tax-2::gfp; srbc-66p::che-13::TagRFP; unc-122p::gfp]</i>	This work
PY8681	<i>oyIs65[str-1p::mCherry]; Ex[str-1p::tax-2::gfp; unc-122p::dsRed]</i>	This work
PY8682	<i>osta-1(ttTi4182) II; oyIs65[str-1p::mCherry]; Ex[str-1p::tax-2::gfp; unc-122p::dsRed]</i>	This work
PY8687	<i>osta-1(ttTi4182) II; kyIs104[str-1p::gfp] X; Ex[str-1::C01B12.4 cDNA:: mCherry; unc-122p::gfp]</i>	This work
PY8693	<i>osta-1(tm5255) II; oyIs14[sra-6p::gfp] V</i>	This work
PY8696	<i>osta-1(tm5255) II; Ex[srbc-64p::srbc-64::gfp; unc-122p::dsRed]</i>	This work
PY8697	<i>osta-1(tm5255) II; Ex[srbc-66p::gfp, unc-122p::dsRed]</i>	This work
PY8698	<i>Ex[srbc-66p::C01B12.4 cDNA::mCherry; srbc-66p::rab-5 cDNA::gfp; unc-122p::gfp]</i>	This work
PY8845	<i>Ex[str-1p::nphp-4 cDNA::gfp; unc-122p::dsRed]</i>	This work
PY9000	<i>osta-1(tm5255) II; Ex[str-1p::tax-2::gfp; unc-122p::dsRed]</i>	This work
PY9001	<i>osta-1(ttTi4182) II; Ex[str-1p::nphp-4 cDNA::gfp; unc-122p::dsRed]</i>	This work
PY9002	<i>osta-1(ttTi4182) II; Ex1[srg-47p::nphp-4 cDNA::gfp; unc-122p::dsRed]</i>	This work
PY9003	<i>osta-1(ttTi4182) II; Ex2[srg-47p::nphp-4 cDNA::gfp; unc-122p::dsRed]</i>	This work
PY9004	<i>Ex3[srg-47p::nphp-4 cDNA::gfp; unc-122p::dsRed]</i>	This work
PY9005	<i>Ex4[srg-47p::nphp-4 cDNA::gfp; unc-122p::dsRed]</i>	This work
PY9006	<i>Ex[str-1p::C01B12.4 cDNA::mCherry; str-1p::nphp-4 cDNA::gfp; unc-122p::gfp]</i>	This work
PY8880	<i>osta-1(ttTi4182) II; Ex1[bbs-8p::mks-2::gfp; osm-5p::xbx-1 cDNA::tdTomato; unc-122p::dsRed]</i>	This work; (Huang et al., 2011)

PY8879	<i>ossta-1(ttTi4182)</i> II; Ex1[ <i>jbtts-14::gfp</i> ; <i>osm-5p::xbx-1::tdTomato</i> ; <i>unc-122p::dsRed</i> ]	(Huang et al., 2011)
DBD234	<i>dpy-23(e840)</i> <i>kyIs104[str-1p::gfp] X</i>	(Kaplan et al., 2012)
FX05517	<i>ossta-2(tm5517)</i>	S. Mitani
FX05460	<i>ossta-3(tm5460)</i>	S. Mitani
UL1983	Ex[F40E10.6p::gfp(fosmid#fUL#CD3); <i>rol-6</i> ]	(Dolphin and Hope, 2006)
MX63	nxEx[ <i>bbs-8p::mks-2::gfp</i> ; <i>osm-5p::xbx-1 cDNA::tdTomato</i> ; <i>rol-6(su1006)</i> ]	(Huang et al., 2011)
MX1099	nxEx[ <i>jbtts-14::gfp</i> ; <i>osm-5p::xbx-1::tdTomato</i> ; <i>rol-6(su1006)</i> ]	(Huang et al., 2011)

**Table S2. Primer sequences**

Primer	Gene	Sequence (5'-3')
AOM477_R4182_2	<i>osta-1</i>	CCATGAGTTGAGAGAATACGAACC
AOM476_R4182	<i>osta-1</i>	GAAATGAGTGCCTACTTGCTCC
AOM196_C01B12.4_F	<i>osta-1</i>	TCCATCAAGAGCATGTCGAG
AOM204_A_nested	<i>osta-1</i>	GGTATGAAAGGTGGCTGTTAG
AOM205_B	<i>osta-1</i>	AGTCGACCTGCAGGCATGCAAGCTTGTGCTGGATTGCGATA
AOM196_C01B12.4_F	<i>osta-1</i>	TCCATCAAGAGCATGTCGAG
AOM204_A_nested	<i>osta-1</i>	GGTATGAAAGGTGGCTGTTAG
AOM249_4_Bfusion	<i>osta-1</i>	AGTCGACCTGCAGGCATGCAAGCTGCTGAAAGTTCAGACTATGA
AOM252_cloning	<i>osta-1</i>	CGCGGATCCATGAAATAGTAAAAACAATCA
AOM253_cloning	<i>osta-1</i>	GGCACCGGTTGCTGGATTGCGATAAAAGAAT
oDBD662	<i>rab-5</i>	GTACCGGT ATGGCCGCCGAAACGCAGGAACCG
oDBD663	<i>rab-5</i>	TTTCCTTTGCGGCCGCTTATTACAGCATGAACCCTTTGT
MW_che-13utrF	<i>che-13</i>	CAAGCATTGAAAGCTCACTTTC
MW_che-13utrR	<i>che-13</i>	GCGCGAAATCAAATCATACAG
MW_tax-2_F_Agel	<i>tax-2</i>	GTACCGGTATGTATCAAGTTCC
MW_tax-2_R_Agel	<i>tax-2</i>	TTTCTACCGGTACATCGGCATGTAGTTCTG
MW_che-13_F_XmaI	<i>che-13</i>	AACCCGGATGGAAGAAGAACACGAAGAAG
MW_che-13_R_Agel	<i>che-13</i>	AAACCGGTATAATGTTAAAAGATTGGCGCTG
srbc-66pR2-BamHI	<i>srbc-66</i>	TCTGAGACACCTGACTTTCTG
srbc-66pF3HindIII	<i>srbc-66</i>	TAAACAGTCACGAAGGCGAG
IVN052	<i>nphp-4</i>	CTTCCCGGGATGTCGGTCAACGACTG
IVN053	<i>nphp-4</i>	CCGACCGGTGAGGAAGCTTCGAATGC
AOM340_C18_pr	<i>osta-2</i>	CACTCCCACATAGGCATTCTCTG
AOM341_C18_Pnest	<i>osta-2</i>	CAAGATATGGCCCGTCAAAG
AOM342_C18_TcB	<i>osta-2</i>	AGTCGACCTGCAGGCATGCAAGCTCCATGGTGAATTTCAGCAT
AOM343_C18_TrB	<i>osta-2</i>	AGTCGACCTGCAGGCATGCAAGCTTAGTGGTCACTCGTCAGTG
AOM336_W0_pr	<i>osta-3</i>	CGTCAGAATGCGGAGAGGTAG
AOM337_W0_Pnest	<i>osta-3</i>	GAGGACTGTGCCTCTATTCAATG
AOM338_W0_TcB	<i>osta-3</i>	AGTCGACCTGCAGGCATGCAAGCTTGTGCTCCTCGCCATTCTG
AOM339_W0_TrB	<i>osta-3</i>	AGTCGACCTGCAGGCATGCAAGCTGTGATCCAGAATCATAGATTGC

**Table S3. Average anterograde and retrograde flux of fusion proteins in the AWB dendrite**

Fusion protein*	Strain background‡	Average number of particles/min ± s.e.§		
		[# kymographs]		
		Anterograde	Retrograde	Stationary
OSTA-1	Wild type	2.2±0.41 [15]	3.5±0.48 [15]	3.0±0.58 [15]
RAB-5	Wild type	29±5.0 [9]	32±4.9 [9]	2.8±0.37 [9]
	<i>osta-1</i>	63±10 [7]¶	60±11 [7]#	2.3±0.63 [7]
RAB-8	Wild type	12±2.9 [8]	22±4.4 [8]	5.8±0.97 [8]
	<i>osta-1</i>	23±3.1 [8]	18±3.0 [8]	7.2±0.71 [8]

Adult animals grown at 25°C were examined.

\*Fusion proteins were expressed under the *str-1* (AWB) promoter.

‡The *osta-1(ttT14182)* allele was used.

§See Materials and methods.

¶Different from corresponding wild-type at  $P<0.01$ .

#Different from corresponding wild-type at  $P<0.05$ .